

Hopping transport of localized π electrons in amorphous carbon films

K. Shimakawa and K. Miyake

*Department of Electronics and Computer Engineering, Faculty of Engineering, Gifu University,
1-1 Yanagido, Gifu 501-11, Japan*

(Received 6 September 1988; revised manuscript received 21 November 1988)

The temperature dependence of the dc and ac conductivities has been studied in sputtered amorphous carbon films. The dc conductivity is proportional to T^n with $n = 15-17$ below room temperature. The mechanism is discussed in terms of the mobility-edge conduction, variable-range hopping, and small-polaron hopping. Quantitatively, these models could not interpret the observed behaviors. Instead, the multiphonon tunneling of localized electrons with weak electron-lattice coupling is suggested to be the dominant transport mechanism. This may be attributed to the π -bonded nature of sputtered amorphous carbon. The ac conductivity is strongly correlated to the dc conductivity, which has never been explained by the current theories based on the pair approximation. Alternatively, the continuous-time random-walk approximation is shown to be a useful approach.

I. INTRODUCTION

It is believed that amorphous carbon (*a*-C) prepared by evaporation or sputtering is predominantly sp^2 bonded with an optical gap of 0.4–0.7 eV.^{1–4} At a carbon sp^2 site, there are three strong σ bonds and one weak π bond lying normal to the σ bonding plane. The π states will form both the valence- and conduction-band states.^{3,4} The sp^2 sites must be clustered together in aromatic units.⁵ The large size of such clusters could produce localized states near the Fermi level E_F .⁵

The effect of disorder in a π -electron system is therefore of particular interest. The present authors⁶ have shown that the temperature dependence of the dc conductivity in sputtered *a*-C is empirically described by $\sigma_{dc} = \sigma_0 T^n$, with $n = 15-17$, which may suggest that the nonpolaronic multiphonon tunneling of localized π electrons (weak coupling with lattice) dominates charge transport.

Measurement of ac conductivity could provide direct information about the hopping rate of localized electrons. In the present study, the temperature dependences of both dc and ac conductivities are reported. Possible transport mechanisms, mobility-edge conduction, variable-range hopping (single-phonon process), and multiphonon hopping with strongly (small-polaron) and weakly coupled states, are discussed. It is suggested that the conventional mobility-edge conduction or small-polaron conduction could not explain the overall features of transport in *a*-C. It is also found that the ac conductivity is strongly correlated with the dc conductivity. This feature, which has never been explained by the current theory based on the pair approximation,⁷ is interpreted well in terms of the continuous-time random-walk (CTRW) approximation.^{8,9}

II. EXPERIMENT

Thin films of *a*-C were prepared on Corning 7059 glass substrate with a bottom Au electrode by rf (13.56-MHz)

sputtering of a 60-mm-diam graphite target (99.999%) in argon gas (0.18 Torr). The forward power applied to the target was 100 W and the substrate was held at 20°C. The deposition rate under these conditions is approximately 0.6 Å/s. Front contacts were made of Au by thermal evaporation. Annealing of samples was done at 400°C (1 h) at 3×10^{-6} Torr. The ac conductivity was measured using a capacitance bridge (Ando TR-1C).

III. EXPERIMENTAL RESULTS AND DISCUSSION

A. dc conductivity

The solid circles in Figs. 1 and 2 show the temperature dependence of dc conductivity (σ_{dc}) for as-deposited and annealed (400°C, 1 h) films of 0.6 μm thickness, respectively. Annealing results in an increase in σ_{dc} , as found by several authors.^{10–12} The activation energy decreases gradually as decreasing temperature, suggesting that the transport mechanisms are thermal activation to the mobility edge at higher temperatures and variable-range hopping at lower temperatures. σ_{dc} for mobility-edge conduction is approximately given by $eN_c\mu_0 \exp(-\Delta E/kT)$, where μ_0 is the microscopic electron mobility and N_c is the effective density of states for the conduction band (carrier is assumed to be electron). ΔE is hard to estimate because there is no good straight line in the $\ln\sigma_{dc}$ versus $1/T$ curve even for higher temperature. Taking, for example, $\Delta E \approx 0.5$ eV for the as-deposited film, and assuming the conventional values of $\mu_0 \approx 10 \text{ cm}^2 \text{ V}^{-1} \text{ s}^{-1}$ and $N_c \approx 10^{19} \text{ cm}^{-3}$, σ_{dc} at 300 K is estimated to be $6 \times 10^{-8} \text{ S cm}^{-1}$, which is about one order larger than the experimentally observed value (see Fig. 1). This suggests that either or both the values of N_c and μ_0 should be considerably smaller than those of assumed values, predicting that the band-edge conduction cannot be dominated by the other transport path. Thermopower (TP) measurement could produce information about the transport path.^{13,14} The small thermopower

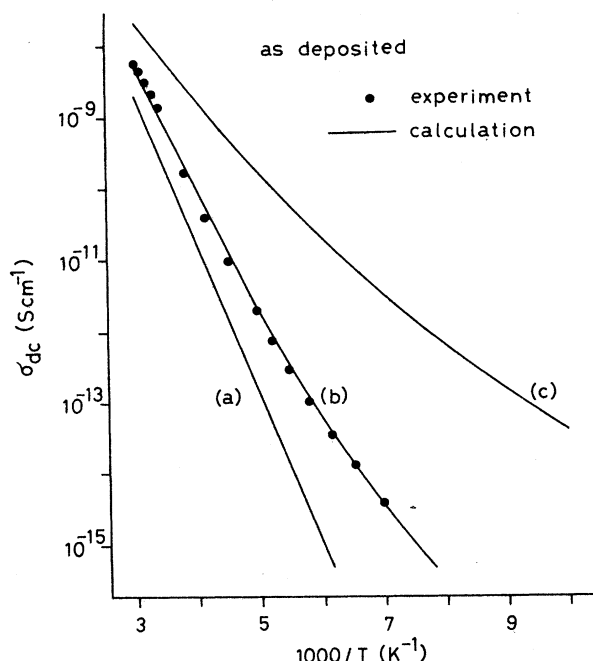


FIG. 1. Temperature dependence of the dc conductivity for the as-deposited a -C film. Solid circles are experimental results and solid lines are calculated results of the nonadiabatic small-polaron hopping.

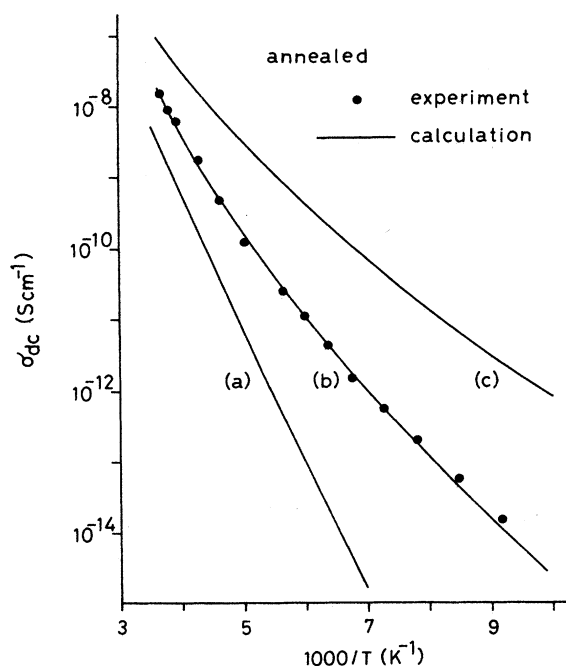


FIG. 2. Temperature dependence of the dc conductivity for the annealed a -C film. Solid circles are experimental results and solid lines are calculated results of the nonadiabatic small-polaron hopping.

(several $\mu\text{V}/\text{deg}$) and the lack of its temperature dependence, which was observed in a -C by Grigorovici *et al.*,¹² suggest that the transport path lies near the Fermi level (not the mobility edge), although TP measurements have not been made in the present films.

Let us check the possibility of transport in localized tail states near the mobility edge. The dc conductivity is written by¹⁴

$$\sigma_{\text{dc}} = e \int g(E) \mu(E) f(E) [1 - f(E)] dE, \quad (1)$$

where $g(E)$ and $\mu(E)$ are energy-dependent density of tail localized states and mobility, and $f(E)$ is the Fermi distribution function. As the $g(E)$ and $\mu(E)$ decrease rapidly whereas $f(E)$ decreases with decreasing energy (toward the Fermi energy E_F), the conduction path shifts toward E_F as the temperature is lowered, yielding nonactivated transport such as is shown in Figs. 1 and 2. However, tail state conduction should also yield large TP and strong temperature dependence of TP. From the above consideration, it is preferred that the transport path lie near E_F in the present a -C.

The localized π states may form a continuous distribution across the band gap and electronic conduction by variable-range hopping¹⁵ ($\ln \sigma_{\text{dc}} \propto T^{-1/4}$) is expected to occur in a -C as in the same manner as tetrahedral a -Ge and a -Si.¹³ It is of interest to examine whether the variable-range hopping predominates dc conduction. The $T^{-1/4}$ plot of dc conductivities for as-deposited (a) and annealed (b) films are shown by open circles in Fig. 3.

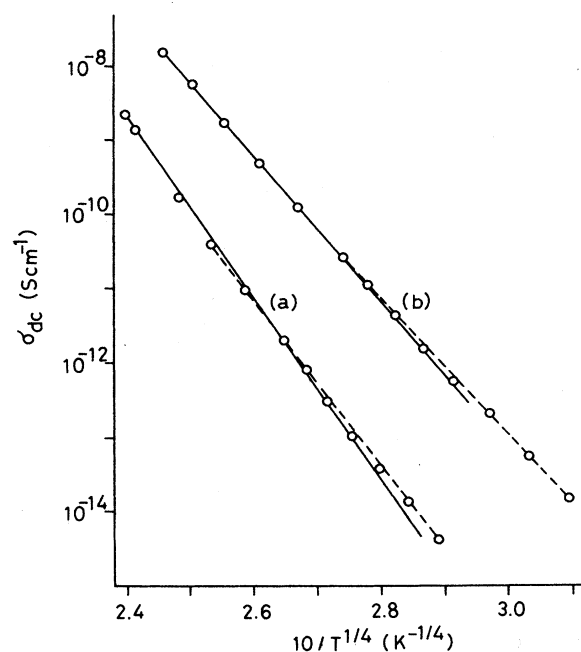


FIG. 3. Temperature dependence of the dc conductivities for (a) as-deposited and (b) annealed a -C films. Temperature scale is $T^{-1/4}$. The fits of variable-range-hopping theory to data at higher temperatures are shown by the solid lines and those at lower temperatures are shown by the dashed lines.

The experimental results are not described by a single straight line over the measured temperature range. The fits to the data at higher temperatures are shown by the solid lines and those at lower temperatures are shown by the dashed lines. It is hard to distinguish from the figure which line (solid or dashed) correctly describes the $T^{-1/4}$ behavior.

The variable-range hopping theory predicts the temperature dependence of σ_{dc} for three-dimensional materials as

$$\ln \sigma_{dc} = A - BT^{-1/4}, \quad (2)$$

where A and B are constants. The theory reproduces many experimental data, particularly for σ -defect amorphous Ge and Si.¹⁵ The parameter B has been used to estimate the density of states at the Fermi level $N(E_F)$, while some difficulties of this theory have been pointed out.^{16,17}

$N(E_F)$ here is estimated from $16\alpha^3/kB^4$, where α^{-1} is the effective Bohr radius of localized electrons and k the Boltzmann constant. Assuming $\alpha^{-1} = 10$ Å, although this value may be smaller than the practical value for a -C because of the delocalized nature of π electrons, $N(E_F)$ for high-temperature fitting (solid lines) is estimated to be 3×10^{16} and 7×10^{16} cm⁻³ eV⁻¹ for as-deposited ($B = 274$ K^{1/4}) and annealed ($B = 224$ K^{1/4}) films, respectively. $N(E_F)$ for low-temperature fitting (dashed lines) is estimated to be 4×10^{16} and 1×10^{17} cm⁻³ eV⁻¹ for as-deposited ($B = 251$ K^{1/4}) and annealed ($B = 204$ K^{1/4}) films, respectively. These values, perhaps an upper limit, seem to be unreasonably small. It is expected that the density of defect is much higher than that of π -defect (10^{18} – 10^{20} cm⁻³ eV⁻¹) a -Ge and a -Si.^{3,4} It is hence suspected that the dc transport cannot be dominated by the variable-range hopping. This may be attributed to weak localization of π defects (large effective α^{-1}): The probability of single-phonon hopping decreases with increasing α^{-1} .¹³

Nonactivated dc transport observed here is similar to that for the small polaron which is formed in the strong electron-lattice coupling.^{18–20} It is of interest to know whether the experimental results can be interpreted in terms of the small-polaron hopping. Before proceeding with the discussion, we summarize the small-polaron hopping theory²⁰ in which both the acoustic and optical phonons are taken into consideration.

In general, the dc hopping conductivity can be given by¹³

$$\sigma_{dc} = n_c (eR)^2 \Gamma_{\min} / 6kT, \quad (3)$$

where n_c is the number of carriers, R the hopping distance, and Γ_{\min} the minimum hopping rate.⁹

If the electron-lattice coupling is strong enough, the small polaron can be formed in disordered materials.¹⁹ Electrons should couple with both the optical and acoustic phonons. Following Holstein,¹⁸ Gorham-Bergeron and Emin²⁰ presented an exact calculation of the nonadiabatic multiphonon transition rate for the small polaron:

$$\begin{aligned} \Gamma = & \left[\frac{J_{ij}}{\hbar} \right]^2 \left[\frac{\hbar^2 \pi}{2(E_c^{\text{op}} + E_c^{\text{ac}})kT} \right]^{1/2} \\ & \times \exp \left[-\frac{\Delta^2}{8(E_c^{\text{op}} + E_c^{\text{ac}})kT} \right] \exp \left[-\frac{\Delta}{2kT} \right] \\ & \times \exp \left[-\frac{E_A^{\text{op}}}{kT} - \frac{E_A^{\text{ac}}}{kT} \right], \end{aligned} \quad (4)$$

where J_{ij} is an electron transfer integral between sites i and j , and Δ the energy difference between sites i and j . E_c^{op} , E_c^{ac} , E_A^{op} , and E_A^{ac} are defined as follows:

$$\begin{aligned} E_c^{\text{op}} &= \frac{\hbar^2}{4kT} \left[\frac{2E_b^{\text{op}}}{\hbar\omega_o} \right] \csc \left[\frac{\hbar\omega_o}{2kT} \right] \omega_o^2, \\ E_c^{\text{ac}} &= \frac{\hbar^2}{4kT} \frac{1}{N} \sum_g \left[\frac{2E_b^{\text{ac}}}{\hbar\omega_{g,\text{ac}}} \right] \csc \left[\frac{\hbar\omega_{g,\text{ac}}}{2kT} \right] \omega_{g,\text{ac}}^2, \\ E_A^{\text{op}} &= \frac{2kT}{\hbar\omega_o} E_b^{\text{op}} \tanh \left[\frac{\hbar\omega_o}{4kT} \right], \\ E_A^{\text{ac}} &= \frac{1}{N} \sum_g \left[\frac{2kT}{\hbar\omega_{g,\text{ac}}} \right] E_b^{\text{ac}} \tanh \left[\frac{\hbar\omega_{g,\text{ac}}}{4kT} \right], \end{aligned} \quad (5)$$

where ω_o is the mean optical frequency (small dispersion of optical mode is assumed here), $\omega_{g,\text{ac}}$ is the acoustic phonon frequency at wave vector g , and N is the number of phonon modes. Two energies, E_b^{op} and E_b^{ac} , are the polaronic binding energies related to optical and acoustic phonons, respectively.

The solid lines, (a), (b), and (c) in Fig. 1, are calculated results using Eqs. (3)–(5). The phonon density of states was approximated to be $g(\nu) \propto \nu^2$ for an acoustic phonon with a cutoff (Debye) frequency ν_D and the mean optical phonon frequency was assumed to be $\nu_o = 3\nu_D$. One of the important physical parameters is the Debye frequency which determines the shape of curve. The curves, Figs. 1(a), 1(b), and 1(c), are for $\nu_D = 2.5 \times 10^{12}$, 5.5×10^{12} , and 1×10^{13} s⁻¹, respectively. The other physical parameters required for calculation are taken to be $E_b^{\text{ac}} = E_b^{\text{op}} = 0.5$ eV, $\Delta = 0.015$ eV, $n_c = 1 \times 10^{18}$ cm⁻³ which is quoted from the electron spin resonance (esr),³ and $R = 5$ Å which may be reasonable for the average site separation of small-polaron hopping. Fitting to experimental data [curve shown in Fig. 1(b)] produces $J_{ij} = 1.0$ eV. It should be noted, however, that estimated J_{ij} (1.0 eV) seems to be very much larger than that (< 0.1 eV) predicted for the nonadiabatic treatment of the small polaron.¹⁸ Beyond this value (≈ 0.1 eV), Eq. (4) cannot be applied to the nonadiabatic small-polaron hopping.²⁰ By assuming $J_{ij} = 0.1$ eV, $n_c = 1 \times 10^{20}$ cm⁻³ is required for fitting, which seems to be too large for the carrier density.

The solid lines, (a), (b), and (c) in Fig. 2, are calculated results for $\nu_D = 3.5 \times 10^{12}$, 7.0×10^{12} , and 1.5×10^{13} s⁻¹, respectively. Other physical parameters used for the calculation are the same as those for as-deposited film. Fitting to experimental data [curve shown in Fig. 2(b)] produces $J_{ij} = 4.5$ eV, which is too large for nonadiabatic

hopping of the small polaron.¹⁸ When $J_{ij}=0.1$ eV is assumed, $n_c=2\times 10^{21}$ cm⁻³ is required, which may also be too large.

The above results suggest that the small polaron could not dominate dc transport in *a*-C, although the qualitative nature is well explained by the small-polaron hopping theory.²⁰ The small polaron cannot be formed when the extent of localized states is larger than the average lattice spacing.^{18,19} The origin of the defect states in a π -electron system should therefore be considered. Robertson⁵ suggested that the deep localized states originated from large π -bonded clusters: The wave function is delocalized across its cluster and the electronic hopping should occur between clusters. The large-radius localized electrons could couple most effectively to long-wavelength (acoustic) phonons ν_0 which are given by $(a_0/\alpha^{-1})\nu_D$, where a_0 is the average lattice spacing.²¹ The delocalized electrons across its cluster will behave as pointlike defects with large α^{-1} . Hence, α^{-1} here should be taken to be cluster size l_c which behaves as "defect." Taking $l_c \approx 60$ Å, which is somewhat arbitrary but is consistent with the prediction by Robertson,⁵ and $\nu_D=390$ K for graphite, $\nu_0 \approx 2 \times 10^{11}$ s⁻¹ ($T_0 = h\nu_0/k \approx 10$ K) is estimated by assuming $a_0 \approx 1.5$ Å. As the binding energy in Eq. (5) under this situation is approximately given by $E_b^{ac}(a_0/l_c)^3$,¹⁹ the electron-lattice coupling is expected to be considerably smaller and hence no small polaron can be formed in *a*-C. It is also believed that the single-phonon hopping process is not expected to occur for such a small ν_0 .^{13,21} We should next consider the multiphonon process with weak-coupling states.

The configurational coordinate diagram for a weak coupling is shown in Fig. 4. The energy E_M in Fig. 4 is the measure of coupling strength. The nonradiative

recombination (phonon emission) rate with weak coupling is given by^{13,22}

$$R(\Delta) = C \exp(-\gamma p) [1 - \exp(h\nu_0/kT)]^{-p}, \quad (6)$$

where $C \approx \nu_0$, $\gamma = \ln(\Delta/E_M) - 1$, and $p = \Delta/h\nu_0$. The multiphonon hopping processes must involve absorption and emission of p phonons. The absorption process is proportional to the Bose factor to the p th power as $[\exp(h\nu_0/kT) - 1]^{-p}$. Under the condition of $h\nu_0 \ll kT$ (high population of phonons), the rate $R(\Delta)$ for the emission will be the same as that for the absorption and is proportional to $(kT/h\nu_0)^p$. Thus Eq. (6) can be applicable to the present hopping problem. The electron overlapping term, which may be given as $\exp(-2\chi R')$, where R' is the actual hopping distance and is roughly given by $R - 2l_c$, and χ is the tunneling parameter, is implicitly included in a constant C . R is the average center-to-center distance between clusters. The parameter γ is the measure of coupling strength. Note that Eq. (6) is similar to the multiphonon jump rate for weak-coupling states derived by Emin¹⁹ (see Appendix). σ_{dc} is obtained from Eqs. (3) and (6). As n_c in Eq. (3) must be given by $N(E_F)kT$ and $R(\Delta)$ here should be Γ_{min} , σ_{dc} is proportional to T^p . The value of p should be an integral number. However, if Δ or ν_0 distributes around a certain mean value, p will be nonintegral.

The same data as Figs. 1 and 2 are replotted on a logarithmic T scale in Fig. 5. Data, Fig. 5(a) for as-deposited and Fig. 5(b) for annealed, are well fitted by the straight lines for all measured temperatures, showing that the logarithmic T plot is better than a $T^{-1/4}$ plot. This shows

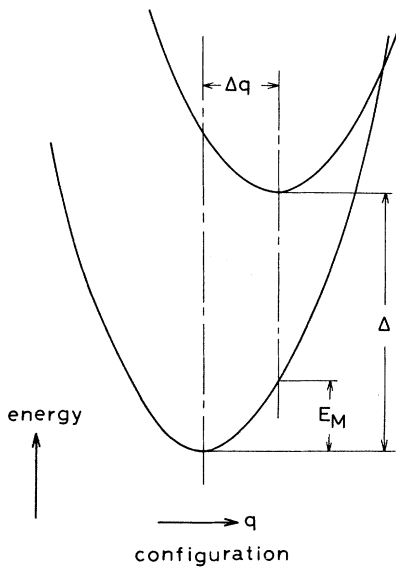


FIG. 4. Configurational coordinate diagram expected for localized states in the weak electron-lattice coupling.

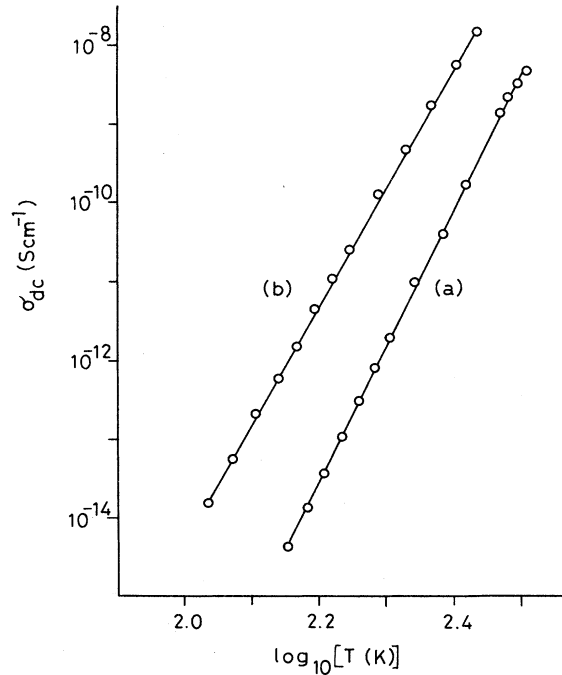


FIG. 5. Logarithmic temperature dependence of the dc conductivities for (a) as-deposited and (b) annealed *a*-C films.

σ_{dc} is proportional to T^n , suggesting that the multiphonon hopping with weak-coupling states dominates electronic transport in *a*-C. The values of n are 17.4 and 15.1 for as-deposited and annealed films, respectively.

B. ac conductivity

Before evaluating physical parameters n_c , R , and Γ_{min} , which appeared in Eq. (3), we turn to ac conductivity which will give information about the hopping rate. The ac conductivity σ_{ac} for many disordered materials can be empirically described by $\sigma_{ac} = Af^s$ at high frequency, where A and s (< 1.0) are usually temperature-dependent parameters.^{23,24} This relation can be interpreted either by the quantum-mechanical tunneling^{25,26} (QMT) or correlated barrier hopping (CBH).²⁷ These models are based on the pair approximation in which the motion of the carrier is contained within a pair of sites. If the dc and ac conductivities arise from the same hopping mechanism, the pair approximation cannot be applied.^{23,24} As the dc conductivity for *a*-C is expected to be dominated by the hopping process, the continuous-time random-walk (CTRW) approximation⁹ originally developed by Scher and Lax⁸ may be the appropriate approach.

In the CTRW, ac conductivity is given as²⁸

$$\sigma(\omega) = K \left[-i\omega + \left\langle \frac{1}{\Gamma + i\omega} \right\rangle^{-1} \right], \quad (7)$$

where K is a constant and $\langle 1/(\Gamma + i\omega) \rangle$ denotes the average over jump frequency distribution $P(\Gamma)$. Under the condition $P(\Gamma) \propto \Gamma^{-1}$, which is encountered in most of the disordered materials,^{23,24} a simple form of ac conductivity is given by⁹

$$\sigma(\omega) = \sigma_{dc} \frac{i\omega\tau}{\ln(1 + i\omega\tau)}, \quad (8)$$

where τ is the maximum hopping time and approximately equal to Γ_{min}^{-1} in Eqs. (3) and (6). It is noted that σ_{ac} is strongly correlated to the dc conductivity. Thus the measurement of ac conductivity could provide knowledge of the hopping rate of localized electrons.

Figures 6 and 7 show the ac conductivity (σ_{ac}) for various temperatures in as-deposited and annealed films, respectively. σ_{ac} is proportional to f^s at higher frequencies, where f is the frequency and s is the temperature-dependent parameter. The observed features are similar to those observed for many amorphous semiconductors.^{23,24} At higher temperatures and lower frequencies, the magnitude of σ_{ac} approaches the dc conductivity σ_{dc} .

As discussed in Sec. III A, dc conduction seems to be dominated by hopping of localized electrons. The ac transport could arise from the same hopping mechanism. To analyze ac conduction for this case, the CTRW approximation must be a proper approach.⁹ The solid lines in Fig. 8 show the calculated σ_{ac} (real part) at 323 K using Eq. (8), where σ_{dc} is set to the experimental value (see frequency-independent conductivity in Fig. 8). The Γ_{min} shown by the arrow is chosen to obtain the best fit, lying close to the onset frequency at which conductivity becomes frequency dependent. The CTRW calculations

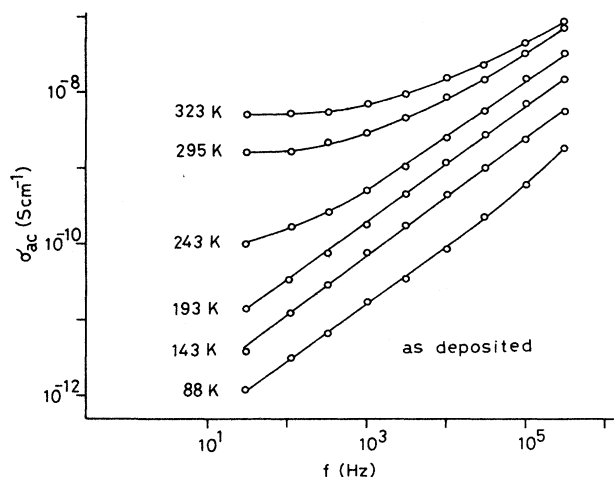


FIG. 6. Frequency-dependent conductivities as a function of temperature for the as-deposited *a*-C film.

agree very well with experimental σ_{ac} at 323 K for both films. Γ_{min} for the annealed film is about one order larger than that for as-deposited film. It is clear that the hopping rate can be estimated from ac conductivity measurement.

Temperature dependence of ac conductivities as a function of frequency for both films is shown in Figs. 9 and 10. Solid circles and solid lines are experimental results and calculations, respectively. σ_{dc} in Eq. (8) is calculated by taking $n_c = N(E_F)kT \approx 1 \times 10^{18} \text{ cm}^{-3}$ at 300 K, which is inferred from the ESR data,³ and $R \approx n_c^{-1/3} \approx 100 \text{ \AA}$. The best fit to as-deposited film is obtained for $\Gamma_{min} = R(\Delta) \approx 2 \times 10^{-23} [T/(10 \text{ K})]^{17.4} \text{ s}^{-1}$. Taking the same n_c and R for annealed film, which must be a valid assumption since the spin density ($10^{18} - 10^{19} \text{ cm}^{-3}$) is relatively independent of annealing,^{2,29} the best

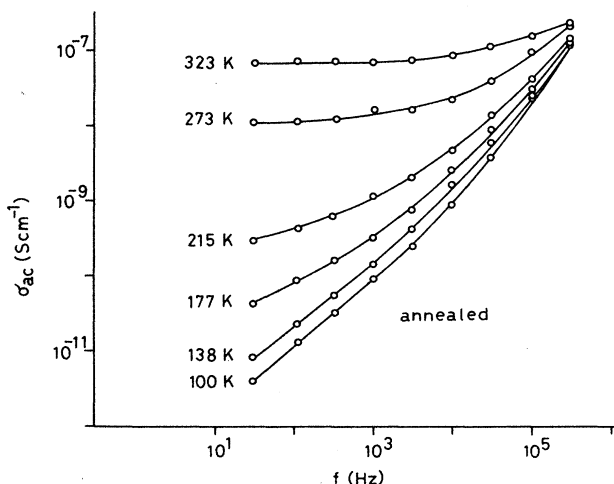


FIG. 7. Frequency-dependent conductivity as a function of temperature for the annealed *a*-C film.

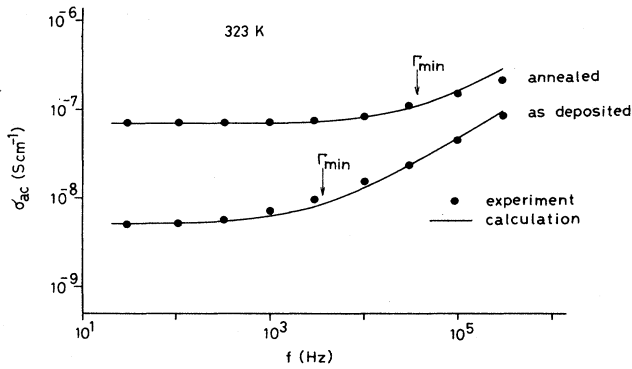


FIG. 8. Calculated (solid lines) and experimental (solid circles) ac conductivities at 323 K for the as-deposited and annealed films. The hopping rate Γ_{\min} [Eq. (6)] is shown by the arrow.

fit to annealed data is obtained for $\Gamma_{\min} \approx 6 \times 10^{-19} [T/(10 \text{ K})]^{15.1} \text{ s}^{-1}$. The calculated results agree with experimental data except for 30 kHz. Disagreement between calculation and experiment at 30 kHz may be due to an onset of quadratic dependence of f on σ_{ac} (see Figs. 6 and 7), which has been usually observed in many amorphous materials around this frequency.^{23,24} It is suggested that the increase in σ_{dc} upon annealing could be due to an increase in multiphonon hopping rate [not due to an increase in $N(E_F)$].

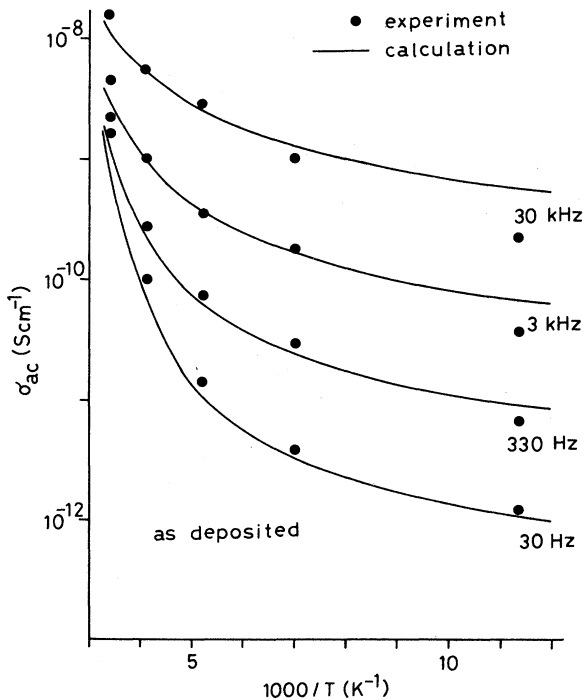


FIG. 9. Temperature dependence of the ac conductivity for the as-deposited *a*-C film. Solid circles are experimental data and solid lines are calculated results.

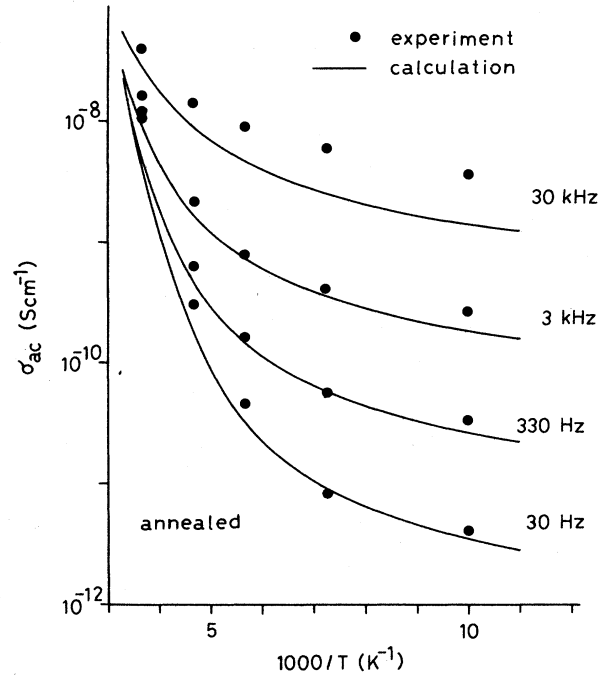


FIG. 10. Temperature dependence of the ac conductivity for the annealed film. Solid circles are experimental data and solid lines are calculated results.

Finally, the physical parameter γ which appeared in Eq. (6) should be made to check the validity of the weak-coupling model. $C \exp(-\gamma p) = 2 \times 10^{-23} \text{ s}^{-1}$ and $6 \times 10^{-19} \text{ s}^{-1}$ for as-deposited and annealed films, respectively, yield the same $\gamma = 4.5$. This γ value is different from $\gamma = 4.1$ in the preceding paper⁶ in which the electron overlapping term was taken into account. As the overlapping term is implicitly included in the constant C , we could neglect this term here. The estimated γ value here may satisfy the weak-coupling condition: Robertson and Friedman²² require the condition of $E_M/h\nu_0 \ll 1$. Englman and Jortner,³⁰ on the other hand, have shown that the weak-coupling regime should satisfy the condition of $G = (E_M/h\nu_0)(kT/h\nu_0) \lesssim 1$. $\gamma = 4.5$ leads to $\Delta/E_M = ph\nu_0/E_M \approx 245$, which provides $E_M/h\nu_0 \approx 0.07$ with $p = 17.4$, yielding $G \approx 2.1$ for 300 K and $G \approx 0.7$ for 100 K. Emin¹⁹ required a more severe condition, $G \ll 1$, for weak-coupling states. However, as will be shown in the Appendix, $G \approx 2$ would still satisfy the weak-coupling condition for relatively large p . Thus we conclude that the multiphonon hopping of localized electrons could dominate electron transport in *a*-C. The increase in σ_{dc} by annealing cannot be due to an increase in the carrier number n_c ,⁷ since the spin density (10^{18} – 10^{19} cm^{-3}) is relatively independent of annealing.^{2,29} This is due to an increase (one order) in the hopping rate Γ_{\min} for annealed film.

IV. CONCLUSIONS

The temperature dependence of dc and ac conductivities were studied in both the as-deposited and annealed

a-C films. The dc conductivity is proportional to T^n , with $n=15-17$ over a wide temperature range. This nonactivated temperature dependence cannot be explained by mobility-edge conduction or variable-range hopping or small-polaron hopping. This might be attributed to the nature of π electrons which are not severely localized. The interaction of a π electron with the lattice can be weak and the nonpolaronic multiphonon process is expected to occur. The ac conductivity is strongly correlated to the dc conductivity and was interpreted in terms of the continuous-time random-walk approximation. It was shown that the hopping rate could be estimated from the CTRW approximation.

ACKNOWLEDGMENTS

The authors would like to thank Professor N. F. Mott for useful comment on a disordered π -electron system. We also wish to thank Dr. D. Emin for comment on the multiphonon process.

APPENDIX

The multiphonon jump rate $R(\Delta)$ of localized electrons coupled to one vibrational mode ω_0 has been derived by Emin:¹⁹

$$R(\Delta) = K \sum_{n=-\infty}^{\infty} [I_p(z) \cos(p\phi_n)] , \quad (A1)$$

$$z = (2E_b / \hbar\omega_0) A_n \operatorname{csch}(\hbar\omega_0 / kT) ,$$

where K is a certain characteristic frequency (probably an order of ω_0), $I_p(z)$ the modified Bessel function given by

$$I_p(z) = (z/2)^p \sum_{k=0}^{\infty} \frac{(z^2/4)^k}{k! \Gamma(p+k+1)} , \quad (A2)$$

and E_b the binding energy (measure of coupling strength), A_n the lattice relaxation amplitude function, and ϕ_n the lattice relaxation-phase shift.

In the weak-coupling limit ($z \simeq 0$), $R(\Delta)$ is given by

$$R(\Delta) \propto [(4E_b / \hbar\omega_0)(kT / \hbar\omega_0)]^p / p! , \quad (A3)$$

where $kT \gg \hbar\omega_0$ is assumed. When p is large, the Stirling formula can be used as²²

$$1/p! \simeq \frac{1}{\sqrt{2\pi p}} p^{-p} \exp(p) .$$

Writing

$$\left[\frac{4E_b}{\hbar\omega_0} \right]^p = \exp \left[\frac{\Delta}{\hbar\omega_0} \ln \left[\frac{4E_b}{\hbar\omega_0} \right] \right]$$

and

$$p^{-p} = (\Delta / \hbar\omega_0)^{-(\Delta / \hbar\omega_0)} = \exp \left[-\frac{\Delta}{\hbar\omega_0} \ln \left[\frac{\Delta}{\hbar\omega_0} \right] \right] ,$$

Eq. (A3) is rewritten as

$$R(\Delta) \propto \exp(-\gamma p) (kT / \hbar\omega_0)^p , \quad (A4)$$

where $\gamma = \ln(\Delta / 4E_b) - 1$. Emin¹⁹ requires the condition of $G = (4E_b / \hbar\omega_0)(kT / \hbar\omega_0) \ll 1$ for weak coupling. However, when p is large (around 15), the small-argument approximation [Eq. (A3)] can still be valid even for $G \simeq 2$ [see Eq. (A2)].

¹J. J. Hauser, *J. Non-Cryst. Solids* **23**, 21 (1977).

²N. Wada, P. J. Gaczi, and R. A. Solin, *J. Non-Cryst. Solids* **35**, 543 (1980).

³J. Robertson, *Adv. Phys.* **35**, 317 (1986).

⁴J. Robertson and E. P. O'Reilly, *Phys. Rev. B* **35**, 2946 (1987).

⁵J. Robertson, *Philos. Mag. Lett.* **57**, 143 (1988).

⁶K. Shimakawa and K. Miyake, *Phys. Rev. Lett.* **61**, 994 (1988).

⁷M. Pollak and T. H. Geballe, *Phys. Rev.* **122**, 1742 (1961).

⁸H. Scher and M. Lax, *Phys. Rev. B* **7**, 4491 (1973).

⁹J. C. Dyre, *Phys. Lett.* **108A**, 457 (1985).

¹⁰C. J. Adkins, S. M. Freake, and E. M. Hamilton, *Philos. Mag.* **22**, 183 (1970).

¹¹M. Morgan, *Thin Solid Films* **7**, 313 (1971).

¹²G. Grigorovici, A. Devenyi, A. Gheorghiu, and A. Belu, *J. Non-Cryst. Solids* **8-10**, 793 (1972).

¹³N. F. Mott and E. A. Davis, *Electronic Processes in Non-Crystalline Materials*, 2nd ed. (Oxford University Press, Oxford, 1979), p. 65.

¹⁴H. Fritzsche, in *Amorphous and Liquid Semiconductors*, edited by J. Tauc (Plenum, London, 1974), p. 221.

¹⁵N. F. Mott, *Philos. Mag.* **19**, 835 (1969).

¹⁶M. H. A. Pramanik and O. Islam, *J. Non-Cryst. Solids* **45**, 325 (1981).

¹⁷M. Ortuno and M. Pollak, *J. Non-Cryst. Solids* **59&60**, 53 (1983).

¹⁸T. Holstein, *Ann. Phys. (N.Y.)* **8**, 343 (1959).

¹⁹D. Emin, *Adv. Phys.* **24**, 305 (1975).

²⁰E. Gorham-Bergeron and D. Emin, *Phys. Rev. B* **15**, 3667 (1977).

²¹D. Emin, *Phys. Rev. Lett.* **32**, 303 (1974).

²²N. Robertson and L. Friedman, *Philos. Mag.* **33**, 753 (1976); **36**, 1013 (1977).

²³A. R. Long, *Adv. Phys.* **31**, 553 (1982).

²⁴S. R. Elliott, *Adv. Phys.* **31**, 135 (1987).

²⁵I. G. Austin and N. F. Mott, *Adv. Phys.* **18**, 41 (1969).

²⁶M. Pollak, *Philos. Mag.* **23**, 519 (1971).

²⁷G. E. Pike, *Phys. Rev. B* **6**, 1572 (1972).

²⁸T. Odagaki and M. Lax, *Phys. Rev. B* **24**, 5284 (1981).

²⁹S. Orzeszko, W. Bala, K. Fabisiak, and F. Rozploch, *Phys. Status Solidi A* **81**, 579 (1984).

³⁰R. Englman and J. Jortner, *Mol. Phys.* **18**, 145 (1970).